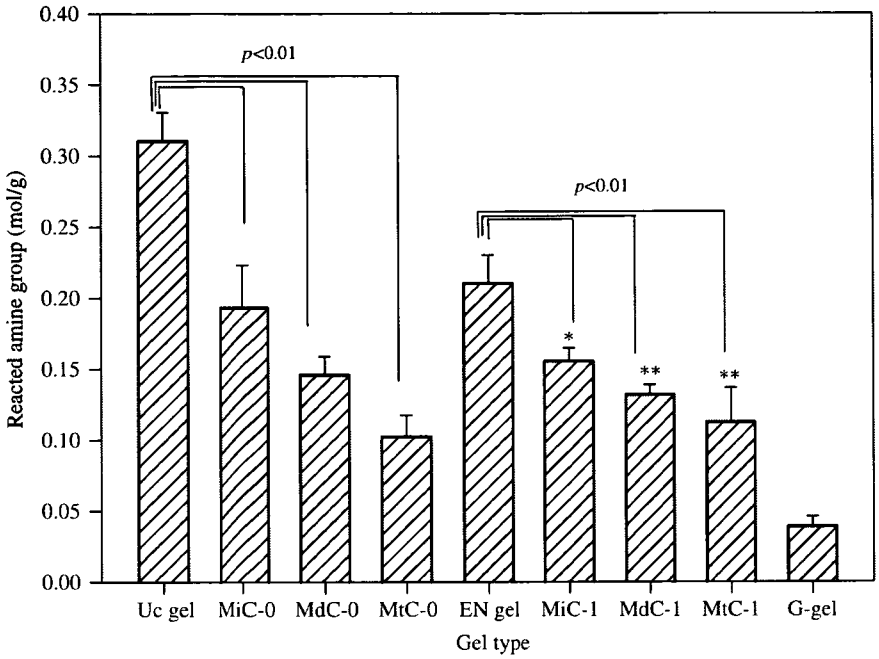

* vs. ** $p < 0.05$

Fig. 3. The percentage of free amine group contents of respective collagen gels. Each value represents the mean ± SD ($n = 5$).

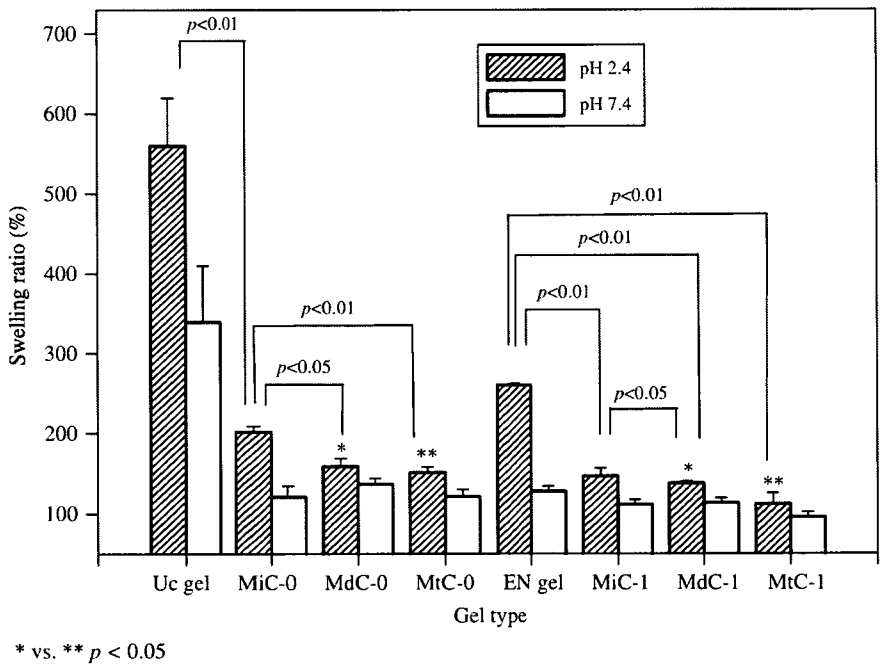

* vs. ** $p < 0.05$

Fig. 4. Swelling ratio of the collagen gels under acidic pH conditions (pH 2.1) (hatched bar) and under neutral pH conditions (pH 7.4) (empty bar). Each value represents the mean ± SD ($n = 5$).

increase decreases as the cross-linking of the collagen gels is proceeded. When assessing the suppression of cell adhesion in terms of intra- and interhelical cross-links, we observed that higher suppression was considerably higher in gels with intra- and interhelical cross-link. MtC-1 gel displayed cell adhesivity that was similar to that of the G-gel.

Cell morphology observed using SEM (Fig. 8) demonstrated that the L929 cells were deformed on the non-MPC surface. On the other hand, the cells remained intact (round) on the CoPho gel surface. An increase in the density of the MPC head group resulted in a decrease in the distribution of L929 cells.

Fig. 9 illustrates the viability of the L929 cells after 48 h. It reveals that cell viability ranges from 96% to 115% (TCPS as 100%) [20]. Cell viability was approximately 70% for the glutaraldehyde cross-linked collagen gel. Immobilization of PMA did not induce any toxicity.

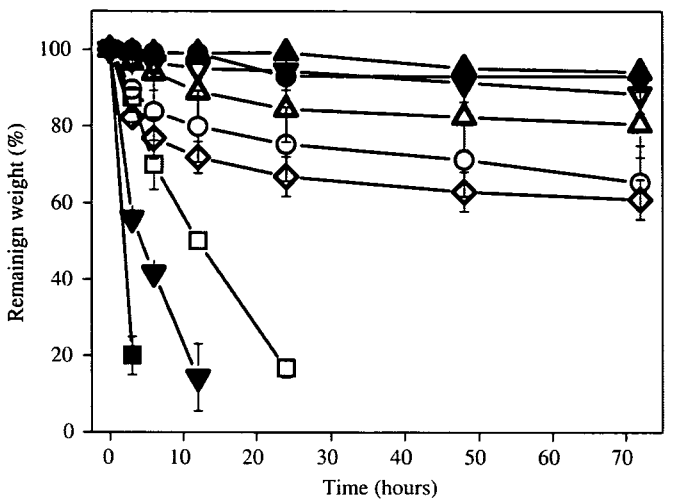

Fig. 5. Degradation of collagen gels by collagenase in Tris–HCl buffer (pH 7.4) at 37 °C. (■) Uc gel, (●) MiC-0 gel, (▲) MdC-0 gel, (▼) MtC-0 gel, (□) EN gel, (○) MiC-1 gel, (△) MdC-1 gel, (▽) MtC-1 gel, and (◇) G-gel. Closed symbols indicate gels without interhelical cross-links while open symbols indicate gels with interhelical cross-links. Each value represents the mean ± SD ($n = 5$).

4. Discussion

4.1. Physical properties of the EN and CoPho gels

The collagen gel that was prepared from a 2 wt% aqueous collagen solution differed from that prepared from a 0.5 wt% collagen solution [11]. A considerably thicker film was obtained (≈ 50 μm), and this film displayed tougher mechanical strength, suppressed swelling, and it slowed collagenase degradation. However, thermodynamic conditions such as shrinkage temperature remained unaltered.

XPS signals displayed a phosphorus peak and a nitrogen peak [$N^+(CH_3)_3$] at 134 and 403.2 eV, respectively; this indicates that PMA was effectively adopted [10,11]. This implies that PMA was successfully immobilized on the surface of the collagen gels. The phosphorus concentration would increase when the MPC is immobilized on the collagen, but did not increase significantly for MtC gels (Table 2). This implies that the immobilization would not occur when the PMA is immobilized for the third time. The increase in the density of the PMA chains is interfering further immobilization process. This can be supplemented by SCA result. The phospholipid head groups on the surface of the collagen gel decreased in the SCA, implying that the surface of the CoPho gel was acquiring a hydrophilic nature (Fig. 2). The hydrophilicty of the CoPho gel was due to the MPC head group, which was located on the surface [18]. The hydrophilic nature of the MPC polymer is thought to be one factor that can suppress

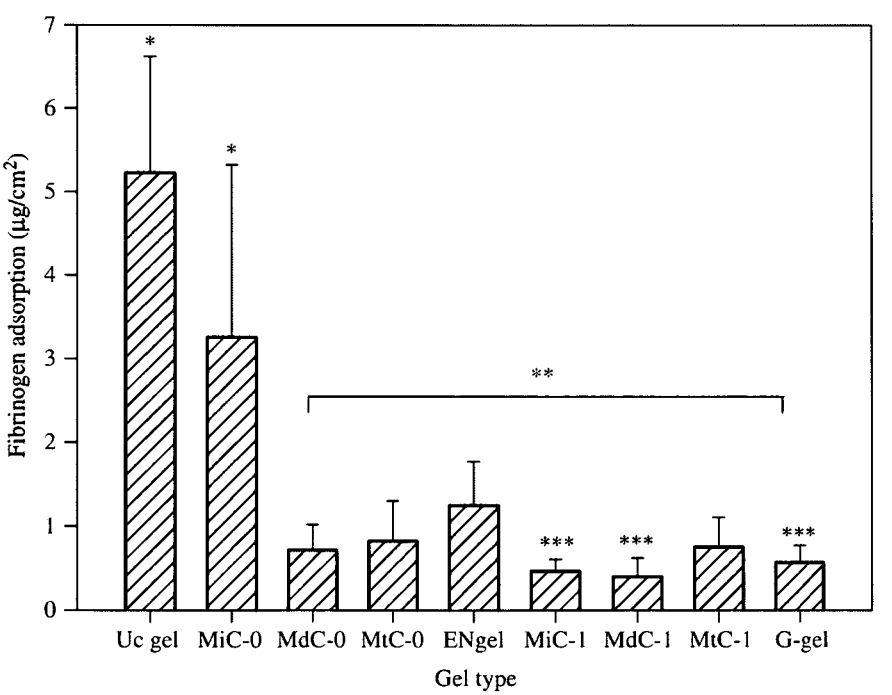

* vs. ** $p < 0.01$
** vs. *** $p < 0.01$

Fig. 6. Fibrinogen adsorption by the collagen gels. Each value represents the mean ± SD ($n = 5$).

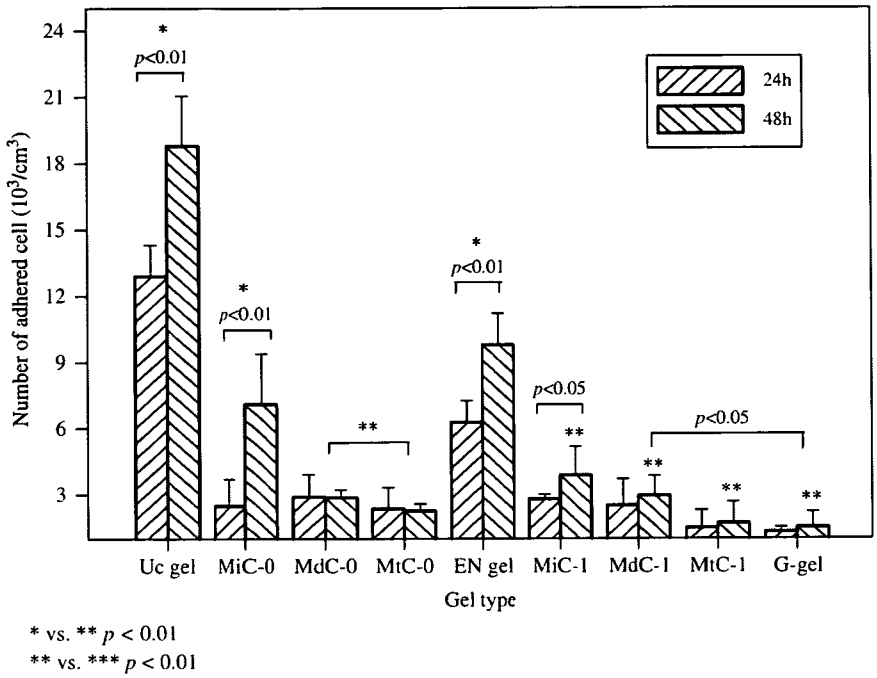

Fig. 7. Cell adhesion property of the respective collagen gels at a seeding density of 5000 cells/cm^2. Each value represents the mean ± SD ($n = 5$).

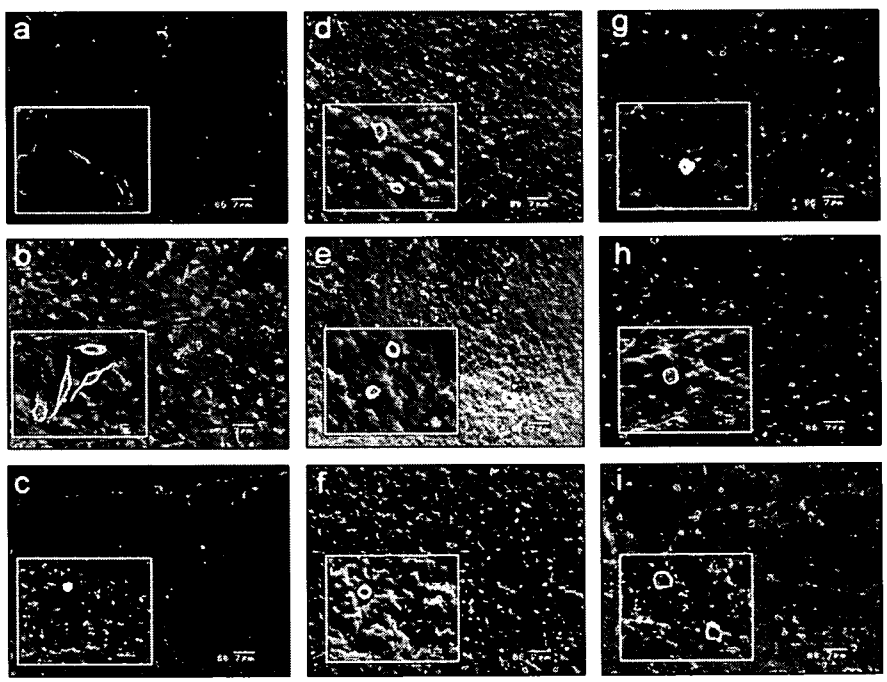

Fig. 8. SEM images of adhered fibroblast cells on respective collagen gels after 48 h of incubation. (a) Uc gel, (b) EN gel, (c) G-gel, (d) MiC-0, (e) MdC-0, (f) MtC-0, (g) MiC-1, (h) MdC-1, and (i) MtC-1 gel. SEM images in the large frame are shown at a magnification of × 150 and the small frame at a magnification of × 1000.

the protein adsorption. It is because the wet condition of the surface is inducing the increase in the mobility of the MPC polymer head group. SCA further decreases as a result of the re-immobilization process, indicating an increase in the density of phospholipid head groups on the surface of the CoPho gels. However, third immobilization process did not decrease the contact angle further.

Did the increase in PMA on the surface of the collagen gel result in a change in the structure of the collagen gels as indicated in Fig. 1? We attempted to characterize the network structure by investigating the reacted amine group content and the swelling ratio (Figs. 3 and 4). Cross-linking collagen gels with EDC/NHS leads to a decrease in the number of reacted amine groups because NH_2 from

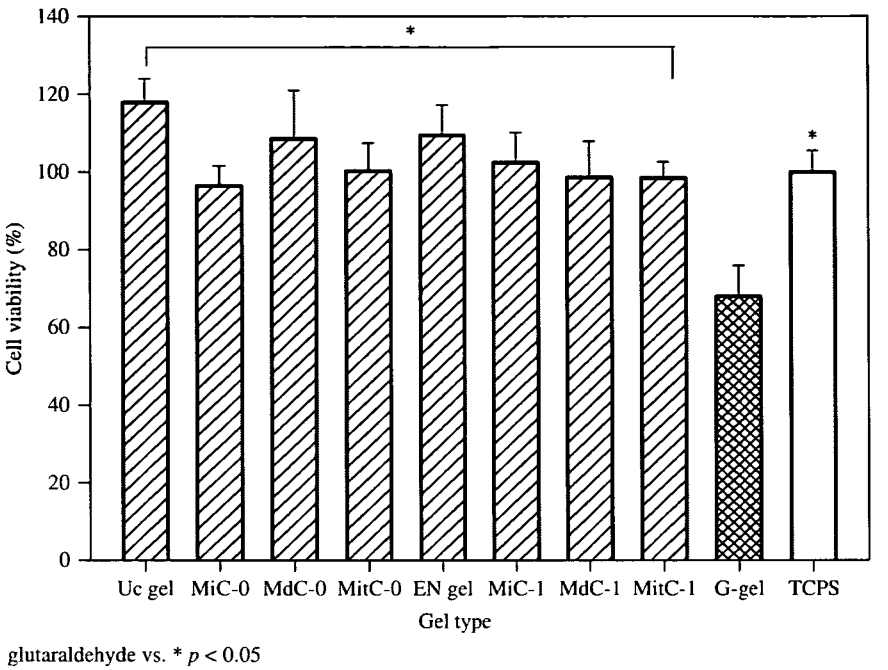

Fig. 9. Cell viability of L929 at 48 h of incubation with at a seeding density of 5000 cells/cm^2 on the respective collagen gels. Each value represents the mean ± SD ($n = 3$).

(hydroxy-)lysine residues is consumed on amide bond formation and NH_3^+ is not formed [7,21]. However, the percentage of the unreacted amine group content was higher than the expected number. Approximately, 60% of the NH_2 remained unreacted compared to Uc gel. Immobilization of PMA on the collagen gel consumed approximately 40% of the amine groups. With regard to PMA immobilization, it is believed that the amine groups may be consumed only on the surface of the collagen gel because PMA cannot penetrate the collagen α-helices [11]. The re-immobilization process decreases the reacted amine group content by up to 40% of Uc gel; immobilization process repeated three times, by up to 30% of Uc gel. The increase in the phosphorus concentration and the decrease in SCA were not observed, but the unreacted amine group content decreased for MtC gels. This implies that the immobilization is stopped, but few intra- and interhelical cross-links have occurred. This decrease is considered high when compared to that of G-gel, which demonstrates approximately 15% of Uc gel. Since the immobilization process occurs only on the surface of collagen gel, lowering the free amine content any further was not possible. An immobilization period of 48 h was the longest period of immobilization that showed a decrease in the number of unreacted amine group, and addition of a higher amount of EDC, NHS, and PMA during the cross-linking process did not cause a significant change in the reacted amine group content (data not shown).

The EN gel is formed by intra- and interhelical cross-links, whereas the CoPho gels are formed by a polymer-helix network. The formation of the cross-link network leads to a decrease in the swelling ratio. In a previous study, we have mentioned that the swelling ratio of the collagen gels is expected to decrease with the progress in cross-linking [11]. The network formed by cross-linking would be dense, and this renders water absorption difficult for the gels. The swelling ratio under acidic and neutral pH conditions varies due to the repulsion force amongst the NH_3^+ and COO^- groups. The swelling ratio is higher for collagen gels immersed in acidic pH condition because they stabilize under neutral pH conditions. With regard to collagen gels prepared with a 0.5 wt% collagen solution, highly acidic pH conditions causes the uncross-linked collagen gels to dissolve [11]; however, none of the collagen gels used in this study dissolved because the α-helices were packed more tightly and were stabilized during gel preparation. Under neutral pH conditions, the collagen film would stabilize by forming a lattice network of fibrils comprising hydrophobic and electrostatic bonds [11,22–24]; hence, the swelling ratio would be less than that observed under acidic pH conditions. The difference in the swelling ratio between the collagen gels with and without inter- and intrahelical cross-links (under acidic pH conditions) is approximately 20–50%. The reacted amine group shows a difference of only 5–10% because stabilization of α-helices by intra- and interhelical cross-links causes a decrease in the swelling ratio. The consumption of carboxyl groups and amine groups is eliminating the site for the protein binding. Arg-Gly-Asp (RGD) site is consumed for the immobilization process, which is making the protein more difficult to adsorbed [25,26]. This would be discussed in Section 4.2.

Formation of a denser network leads to difficulties in the degradation by collagenase (Fig. 5). Activation of collagenase requires adsorption on the collagen gel surface [11,27]. Subsequently, the collagenase penetrates the collagen gel and begins to cleave the helices [28]. However, a low swelling ratio does not permit collagenase absorption by the CoPho gels. The degradation rate is considerably slower due to an increase in PMA density. A high density of phospholipid head groups is believed to prevent collagenase adsorption on the surface. Eventually, the CoPho gels would be more stable against collagenase.

4.2. Biological properties of EN and CoPho gels

As previously mentioned, the hydrophilicity of the CoPho gel increases with immobilization of PMA due to the presence of phospholipid head group on the CoPho gel. High hydrophilicity is known to be one of the factors that lead to difficulties in protein adsorption [29]. Increase in the density of PMA results in a decrease in the adsorption rate of fibrinogen (Fig. 6). This implies that the immobilized MPC polymer leads to difficulties in the interaction of proteins with the gel surface. In addition to this, the cross-links also decrease protein adsorption. The ε-amino groups from (hydroxy-)lysine residues of collagen are blocked by the cross-linking process [30]. Thus, it is believed that hydrophilicity of the hybrid gel and the blocked ε-amino group renders it difficult for the hybrid gel surface to adsorb fibrinogen. A similar phenomenon was observed during the cell adhesion test (Fig. 7). We observed that repeated immobilization of PMA suppressed cell adhesion. Comparison of cell adhesion after 24- and 48-h cycles revealed that the number of adhered cells in the case of the Uc gel after 48 h cycle had increased by approximately 2 times; this rate of increase would decrease as collagen gels more phospholipids is immobilized. Immobilization of PMA did not induce any toxicity. Decrease in cell attachment on CoPho gels was entirely attributable to the surface property, i.e., the ability to regulate cell adhesion and protein adsorption. These results indicate that the immobilization of the PMA would induce almost the same effect as that of G-gel but without toxicity. As mentioned in Section 4.1, the formation of the cross-linking is eliminating the site for the protein binding. Same affect can be expected for the G-gels. Consumption of RGD for the cross-linking is making the gels to resist against protein adsorption and cell adhesion. Improper cross-linking by glutaraldehyde would induce the high protein adsorption [25]. However, in our case, G-gel showed low protein adsorption and cell adhesion, indicating that the RGD is effectively cross-linked. The formation of the cross-link is bringing the difficulty in the adsorption of proteins.

When assessing suppression of cell adhesion in terms of intra- and interhelical cross-links, we observed that suppression was considerably higher in gels with intra- and interhelical cross-links. The MtC-1 gel displayed cell adhesivity that was similar to that of the G-gel. This implies that intra- and interhelical cross-links also constitute an important parameter in suppression of cell adhesion. This can be reaffirmed by the fact that the number of cells adhered onto the EN gel is less than that in the case of the Uc gel. Much higher affect can be seen for G-gel, but we could not detect high suppression of cell adhesion by EDC/NHS cross-link, indicating that the functional groups still exist largely on the surface. Comparing EN gel and MiC-0 gel, the reacted amine group content is almost the same but the biological property is different. This is due to the difference in the surface property of the EN gel and MiC-0 gel. Investigation of cell morphology revealed that the L929 cells were deformed on the non-MPC surface (Fig. 8). On the other hand, the cells remained intact (round) on the surface of the CoPho gels, indicating a weak interaction between cells and the surface [19]. However, the adsorption of protein and the adhesion of the cell were still higher compared to other materials that used MPC polymer [18,31–33]. Ishihara et al. pointed out that 30 mol% of MPC polymer is required for fibroblast suppression [29]. Repeated immobilization increased the number of phosphorylcholine moieties on the surface of collagen gel surface. However, it is believed that the increase in the number of phospholipids moieties is no longer possible, and no significant decrease was observed in the amount of adsorbed fibrinogen and adhered cells.

5. Conclusion

Repeated immobilization of PMA can increase its immobilization rate, resulting in an increase in the number of MPC head groups; hence, unreacted amine group content and the swelling ratio decreased and the degradation by the collagenase was delayed. The cell morphology remained round indicating a weak interaction between the cells and the gel surface. Thus, the CoPho gel can be used as an alternative collagen-based gel for an implantable biomedical device. Furthermore, we expect that co-immobilization with different polymer-possessing carboxyl groups such as heparin is possible. In the near future, we look forward to reporting on the use of the CoPho gel *in vivo*.

Acknowledgments

This study was financially supported by a grant from the Research on Health Sciences focusing on Drug Innovation (KH61060) from the Japan Health Sciences Foundation and a grant from the Health and Labour Sciences Research Grants.

We would like to thank Dr. Kazuhiko Ishihara of The University of Tokyo for his kind assistance and advice on the preparation and analysis of the MPC polymer and Mr. James Sibarani of The University of Tokyo for his assistance on XPS analysis.

References

[1] Friess W. Collagen-biomaterials for drug delivery. Eur J Pharm Biopharm 1998;45:112–36.

[2] Nimni ME, Cheung D, Strates B, Kodama M, Sheikh K. Chemically modified collagen: a natural biomaterial for tissue replacement. J Biomed Mater Res 1987;21:741–71.

[3] Zeeman R, Dijkstra PJ, van Wachem PB, van Luyn MJ, Hendriks M, Cahalan PT, et al. Successive epoxy and carbodiimide cross-linking of dermal sheep collagen. Biomaterials 1999;20:921–31.

[4] Yoshizato K, Nishikawa A, Taira T. Functionally polarized layers formed by epidermal cells on a permeable transparent collagen film. J Cell Sci 1988;91:491–9.

[5] Weadock KS, Miller EJ, Bellincampi LD, Zawadsky JP, Dunn MG. Physical crosslinking of collagen fibers: comparison of ultraviolet irradiation and dehydrothermal treatment. J Biomed Mater Res 1995; 29:1373–9.

[6] Barbani N, Lazzeri L, Cristalli C, Cascone MG, Polacco G, Pizzirani G. Bioartificial materials based on blends of collagen and poly(acrylic acid). J Appl Polym Sci 1999;72:971–6.

[7] Olde Damink LHH, Dijkstra PJ, van Luyn MJA, van Wachem PB, Nieuwenhuis P, Feijen J. Cross-linking of dermal sheep collagen using a water-soluble carbodiimide. Biomaterials 1996;17:765–73.

[8] Wissink MJB, Beernink R, Pieper JS, Poot AA, Engbers GHM, Beugeling T, et al. Immobilization of heparin to EDC/NHS-cross-linked collagen. Characterization and in vitro evaluation. Biomaterials 2001;22:151–63.

[9] van Luyn MJA, van Wachem PB, Olde Damink LHH. Relations between in vitro cytotoxicity and cross-linked dermal sheep collagens. J Biomed Mater Res 1992;26:1091–110.

[10] Ishihara K, Nomura H, Mihara T, Kurita K, Iwasaki Y, Nakabayashi N. Why do phospholipid polymers reduce protein adsorption? J Biomed Mater Res 1998;39:323–30.

[11] Nam K, Kimura T, Kishida A. Preparation and characterization of cross-linked collagen-phospholipid polymer hybrid gels. Biomaterials 2007;28:1–8.

[12] Wissink MJB. Endothelialization of collagen matrices. Doctor's thesis, University of Twente, 1999; Chapter 4, p. 61–86.

[13] Nam K, Watanabe J, Ishihara K. Characterization of the spontaneously forming hydrogels composed of water-soluble phospholipid polymers. Biomacromolecule 2002;3:100–5.

[14] Olde Damink LH, Dijkstra PJ, Van Luyn MJ, Van Wachem PB, Nieuwenhuis P, Feijen J. Changes in the mechanical properties of dermal sheep collagen during in vitro degradation. J Biomed Mater Res 1995;29:139–47.

[15] Bubnis WA, Ofner III. CM. The determination of ε-amino groups in soluble and poorly soluble proteinaceous materials by a spectrophotometric method using trinitrobenzenesulfonic acid. Anal Biochem 1992;207:129–33.

[16] Everaerts F, Torrianni M, van Luyn M, van Wachem P, Feijen J, Hendriks M. Reduced calcification of bioprostheses, cross-linked via an improved carbodiimide based method. Biomaterials 2005;25: 5523–30.

[17] Higuchi A, Sugiyama K, Yoon BO, Sakurai M, Hara M, Sumita M, et al. Serum protein adsorption and platelet adhesion on pluronict-adsorbed polysulfone membranes. Biomaterials 2003;24:3235–45.

[18] Goda T, Konno T, Takai M, Moro T, Ishihara K. Biomimetic phosphorylcholine polymer grafting from polydimethylsiloxane surface using photo-induced polymerization. Biomaterials 2006;27:5151–60.

[19] Watanabe J, Ishihara K. Phosphorylcholine and poly(D,L-lactic acid) containing copolymers as substrate for cell adhesion. Artif Organs 2003;27:242–8.

[20] Lin Y, Wang L, Zhang P, Wang X, Chen X, Jing X, et al. Surface modification of poly(L-lactic acid) to improve its cytocompatibility via assembly of polyelectrolytes and gelatin. Acta Biomater 2006;2: 155–64.

[21] Khara AR, Peppas NA. Swelling/deswelling of anionic copolymer gels. Biomaterials 1995;16:559–67.

[22] Ripamonti A, Roveri N, Briga D. Effects of pH and ionic strength on the structure of collagen fibrils. Biopolymers 1980;19:965–75.

[23] Wallace D. The relative contribution of electrostatic interactions to stabilization of collagen fibrils. Biopolymers 1990;29:1015–26.

[24] Rosenblatt J, Devereux B, Wallace D. Dynamic rheological studies of hydrophobic interactions in injectable collagen biomaterials. J Appl Polym Sci 1993;50:953–63.

[25] Ber S, Köse T, Hasırcı V. Bone tissue engineering on patterned collagen films: and in vitro study. Biomaterials 2005;26:1977–86.

[26] Chandy T, Das GS, Wilson RF, Rao GHR. Use of plasma glow for surface-engineering biomolecules to enhance blood compatibility of Dacron and PTFE vascular prosthesis. Biomaterials 2000;21: 699–712.

[27] Everaerts F, Torrianni M, van Luyn M, van Wachem P, Feijen J, Hendriks M. Reduced calcification of bioprostheses, cross-linked via an improved carbodiimide based method. Biomaterials 2005;25: 5523–30.

[28] Ma L, Gao C, Mao Z, Zhou J, Shen J. Enhanced biological stability of collagen porous scaffolds by using amino acids as novel cross-linking bridges. Biomaterials 2004;25:2997–3004.

[29] Ishihara K, Ishikawa E, Iwasaki Y, Nakabayashi N. Inhibition of fibroblast cell adhesion on substrate by coating with 2-methacryloyloxyethyl phosphorylcholine polymers. J Biomater Sci Polym Edn 1999;10:1047–61.

[30] Hersel U, Dahmen C, Kessler H. RGD modified polymers: biomaterials for stimulated cell adhesion and beyond. Biomaterials 2003;24:4385–415.

[31] Yamasaki A, Imamura Y, Kurita K, Iwasaki Y, Nakabayashi N, Ishihara K. Surface mobility of polymers having phosphorylcholine groups connected with various bridging units and their protein adsorption-resistance properties. Colloids Surf B: Biointerf 2003;28:53–62.

[32] Watanabe J, Ishihara K. Cell engineering biointerface focusing on cytocompatibility using phospholipid polymer with an isomeric oligo(lactic acid) segment. Biomacromolecules 2005;6:1797–802.

[33] Goda T, Konno T, Takai M, Moro T, Ishihara K. Photoinduced phospholipid polymer grafting on Parylene film: advanced lubrication and antibiofouling properties. Colloids Surf B: Biointerfaces 2007;54:67–73.

CONTROLLED RELEASE SOCIETY

Volume 24•Number 2•2007

NEWSLETTER

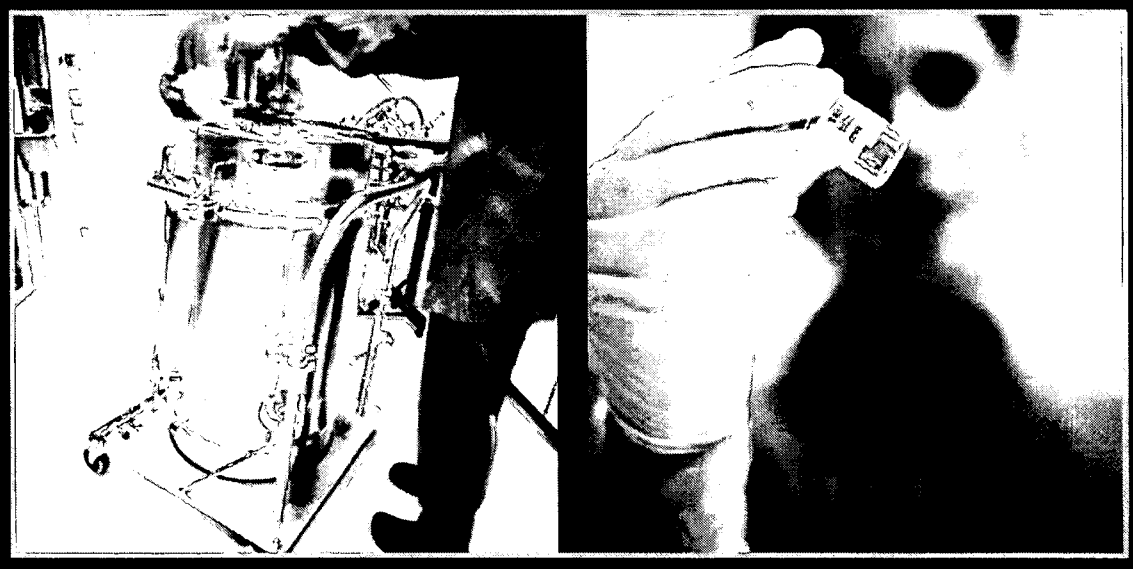

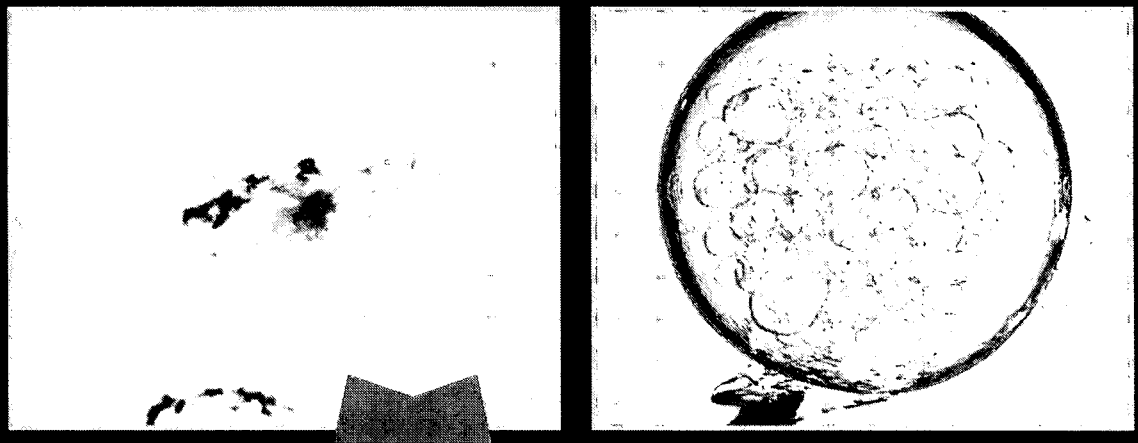

Scientifically Speaking

Gene Transfection on Tissue Engineered Bone Decellurized by Ultra-High Hydrostatic Pressurization

By Tsuyoshi Kimura, Seiichi Funamoto and Akio Kishida
Institute of Biomaterials and Bioengineering
Tokyo Medical and Dental University, Tokyo, Japan

Introduction

The development of scaffold, which contributes to adhesion and expansion of cells that can regenerate tissue lost to disease, is one of the key factors in tissue regeneration. Many researchers have investigated polymeric scaffolds, such as poly(lactic acid) (1), poly(glycolic acid) (2), hyaluronic acid (3), and collagen (4). It has been reported that the shape and microscopic structure of these scaffolds, such as porous, fibrous, and gel, plays an important role in tissue formation, as does the physical and physicochemical nature of the scaffold (5). However, it is difficult to obtain the same shape and structure as the biological tissue. Therefore, there is an alternate approach for preparing scaffold that is similar to the natural scaffold that uses decellularized tissues from which the cells and antigen molecules have been removed to diminish the host immune reaction. The decellularized scaffold is thought to have the same structure and composition as the natural tissue, and the regeneration within the scaffold is expected to be regulated by donor cells. Detergents, such as Triton® X-100 (6), sodium dodecyl sulfate (7), and sodium cholate (8), generally are used to remove the donor cells and their components. The remainder of the detergents, the residual cellular component in the scaffold, and the denaturing of tissue are reported to be important problems. We have also reported on the development of tissue engineered bone by novel physical decellularization process using ultra-high pressure (UHP) technology without surfactant (9). This decellularization method involves two processes. As a first step, cells, bacteria, and viruses in the tissue are disrupted by ultra-high pressurization. Subsequently, the residues of disrupted cells are removed by washing (Figure 1).

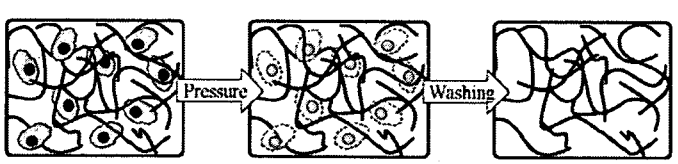

Figure 1. Preparation procedure for decellularizing tissue using ultra-high pressure treatment.

Recently, the focus has been the combination of tissue engineering scaffold and gene therapy, which provide the physical support for cell adhesion and cellular functioning by delivering the gene (10). For *in vitro* gene delivery, non-viral vectors, such as cationic polymers, cationic lipids (11), and calcium phosphate (12), have been used for stabilization of DNA, resulting in effective gene transfection. On the other hand, when they are applied in a living body, their cytotoxicity and low transfection efficiency likely will become considerable problems. For bone regeneration, it is thought that calcium phosphate, which is one component of bone, is suitable as a gene carrier because it is able to form a co-precipitate with DNA for gene transfection and to become bone by itself.

In this study, we demonstrated the preparation of decellularized bone by pressurization and gene transfection to reseeded cells on the decellularized bone with co-precipitates of calcium phosphate with plasmid DNA *in vitro*.

Results

Porcine bones (femur and costa) were cut and shaped and then pressurized at 25°C and 10,000 atm (980 MPa) for 10 min (UHP treatment). After UHP treatment, they were washed by culture medium containing DNase I at 37°C for 2 weeks. The decellularization of bone was evaluated by hematxylin and eosin (H-E) staining. Figure 2 shows that the removal of cells in bone and bone marrow of femur was completely achieved by UHP treatment. The porous structure of bone and the fibrous structure of collagen, along with lipid droplets in bone marrow, were well maintained. The decellularized costa also was prepared by UHP treatment. MC3T3 cells (1×10^5 cells) were reseeded on the decellularized bone *in vitro*. After cultivation for 3 days, the

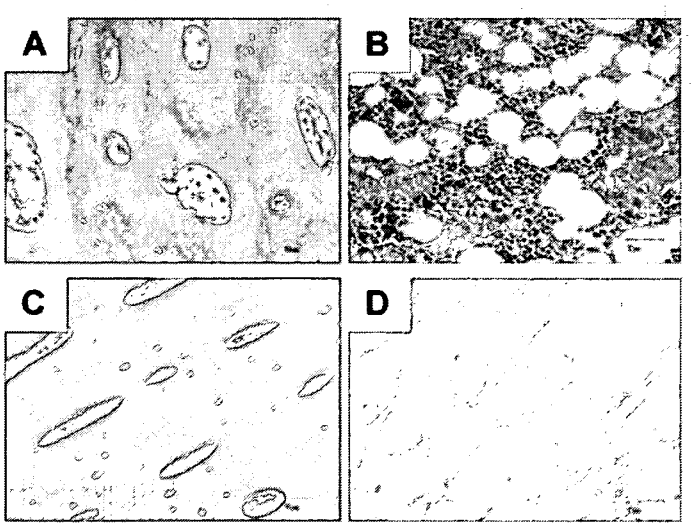

Figure 2. Hematoxylin eosin staining of (A) native cortical bone, (B) native bone marrow, (C) decellularized cortical bone, and (D) decellularized bone marrow by pressurization at 10,000 atm (980 MPa) for 10 min.

adhesion and extension of cells on the surface of the decellularized bone was observed at the outside and the inside of the bone under scanning electronic microscopy (SEM). The decellularized femur was implanted subcutaneously in rats to investigate their biocompatibility. After 2- and 4-weeks implantation, they were explanted and subjected to histological study (H-E staining). Light microscopic observation confirmed that a strong inflammatory response was observed on native bone after 2 weeks. Fibrous encapsulation and gradual collapse of bone marrow occurred after 4 weeks. On the other hand, very thin fibrous encapsulation was observed around the decellularized femur. The re-construction of tissue by infiltration of cells in decellularized bone marrow also was observed after 4 weeks, suggesting the capability of the decellularized bone as a bio-scaffold.

Plasmid DNA encoding beta-galactositase gene under cytomegarovirus promoter (pCMV-beta: clonetech) was used. A solution of pCMV-beta was mixed with $CaCl_2$ solution (*2M*) and added to 2× HBS solution to form the co-precipitate of pCMV-beta and calcium phosphate. The decellularized bone was immersed in the mixture at 37°C for 30 min. MC3T3 cells (5×10^4 cells) were reseeded on the decellularized bone and cultivated for 3 days. The gene transfection was evaluated by X-gal staining. Without co-precipitation, there was no change in cells reseeded on the decellularized bone with only DNA, whereas blue-stained cells were observed on the decellularized bone with calcium/DNA co-precipitate (Figure 3), indicating effective gene expression by the combination of the calcium phosphate co-precipitate method and tissue engineered bone. This result indicated that decellularized tissue was significantly useful in the novel combination of the tissue engineered scaffold and gene delivery.

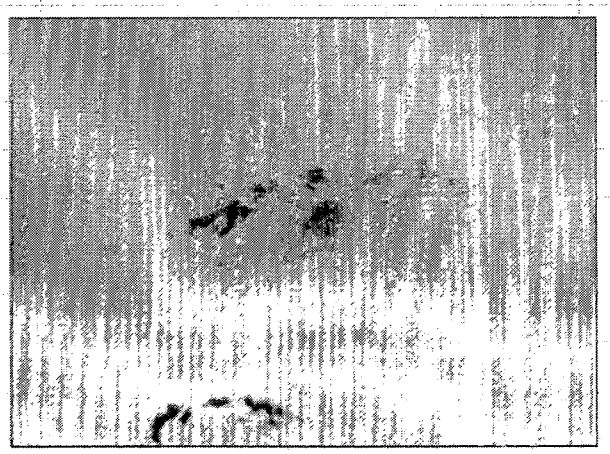

Figure 3. X-gal staining of cells reseeded on decellularized costa with calcium phosphate/DNA co-precipitate.

Conclusions

Porcine bones (femur and costa) were decellularized successfully using UHP and washing processes. The decellularized tissue would be useful in bone tissue regeneration. The decellularized bone also acted as a gene delivery/transfectioning matrice for the cells incorporated to the bone. Combining a decellularized tissue and gene delivery system is expected to be a useful technology for regenerating tissue, not only bones but also other tissues, such as blood vessels, skin, and heart muscles.

References

1. Middleton, JC, Tipton, AJ. Synthetic biodegradable polymers as orthopaedic devices, Biomaterials 21: 2335-2346 (2000).
2. Ameer, GA, Mahmood, TA, Langer, R. A biodegradable composite scaffold for cell transplantation, J. Orthop. Res. 20: 16-19 (2002).
3. Ji, Y, Ghosh, K, Shu, XZ, Li, B, Sokolov, JC, Prestwich, GD, Clark, RA, Rafailovich, MH. Electrospun three-dimensional hyaluronic acid nanofibrous scaffolds, Biomaterials 27: 3782-3792 (2006).
4. Lee, SJ, Lim, GJ, Lee, JW, Atala, A, Yoo, JJ. In vitro evaluation of a poly(lactide-co-glycolide)-collagen composite scaffold for bone regeneration, Biomaterials 27: 3466-3472 (2006).
5. Chen, G, Ushida, T, Tateishi, T. Scaffold design for tissue engineering, Macromol. Biosci. 2: 67-77 (2002).
6. Bader, A, Schilling, T, Teebken, OE, Brandes, G, Herden, T, Steinhoff, G, Haverich, A. Tissue engineering of heart valves—Human endothelial cell seeding of detergent acellularized porcine valves, Eur. J. Cardio. Thorac. Surg. 14: 279-284 (1998).
7. Grauss, RW, Hazekamp, MG, van Vliet, S, Gittenberger-de Groot, AC, DeRuiter, MC. Decellularization of rat aortic valve allografts reduces leaflet destruction and extracellular matrix remodeling, J. Thorac. Cardiov. Surg. 126: 2003-2010 (2003).
8. da Costa, FDA, Dohmen, PM, Lopes, SV, Lacerda, G, Pohl, F, Vilani, R, da Costa, MBA, Vieira, ED, Yoschi, S, Konertz, W, da Costa, IA. Comparison of cryopreserved homografts and decellularized porcine heterografts implanted in sheep, Artif. Organs 28: 366-370 (2004).
9. Fujisato, T, Minatoya, K, Yamazaki, S, Meng, Y, Niwaya, K, Kishida, A, Nakatani, T, Kitamura, S. Preparation and recellularization of tissue engineered bioscaffold for heart valve replacement, In, Mori, H, Matsuda, H, (eds), Cardiovascular Regeneration Therapies Using Tissue Engineering Approaches, Springer-Verlag, Tokyo, Japan, pp83-94 (2005).
10. Jang, JH, Shea, LD. Controllable delivery of non-viral DNA from porous scaffolds, J. Control. Release 86: 157-168 (2003).
11. Zhang, SB, Xu, YM, Wang, B, Qiao, WH, Liu, DL, Li, ZS. Cationic compounds used in lipoplexes and polyplexes for gene delivery, J. Control. Release 100: 165-180 (2004).
12. Roy, I, Mitra, S, Marita, A, Mozumdar, S. Calcium phosphate nanoparticles as non-viral vectors for target gene delivery, Int. J. Pharm. 250: 25-33 (2005).

Nucleic Acids Symposium Series No. 51 343–344
doi:10.1093/nass/nrm172

Characteristics of compacted plasmid DNA by high pressurization

Tsuyoshi Kimura[1], Kana Horiuchi[2], Kimio Kurita[2], Tsutomu Ono[3], Hidekazu Yoshizawa[3], Toshiya Fujisato[4], Akio Kishida[1]*

[1]Institute of Biomaterials and Bioengineering,Tokyo Medical and Dental University, 2-3-10 Kanda-surugadai, Chiyoda-ku, Tokyo, Janan, [2]Callege of Science and Technology, Nihon University, 1-8-14 Kanda-surugadai, Chiyada-ku, Tokyo, Japan, [3]Guraduate school of Environmental Science, Okayama University, 3-1-1 Tsushima-naka, Okayama, Japan and [4]Department of Biomedical Engineering, Osaka Institute of Technology, 5-16-1 Omiya, Asahi-ku, Osaka, Japan.

ABSTRACT

In order to investigate the effect of pressure on the tertiary structure of plasmid DNA having the super-coiled and relaxed forms, the solution of plasmid DNA was hydrostatically pressurized at different atmosphere and 40°C for various times. For dynamic light scattering (DLS) measurement of the pressurized plasmid DNA, the hydrodynamic diameters of the super-coiled and relaxed plasmid DNA were decreased with increasing pressure. Also, at constant pressure, a long period of pressure treatment effectively induced the decrease in plasmid DNA. These results suggest that the plasmid DNA was condensed by high hydrostatic pressurization. The circular dichroism (CD) spectrum of the pressurized plasmid DNA was slightly changed. For digestion by S1 nuclease, which selectively cleaves single strand DNA, the pressurized plasmid DNA was easily degraded compared to the non-pressurized plasmid DNA, suggesting that the double helix of plasmid DNA was partly dissociated to single strand by the pressure-induced compaction of plasmid DNA. These results indicate that high hydrostatic pressurization is one of powerful tools for preparing the compacted plasmid DNA.

INTRODUCTION

Plasmid DNA was utilized for gene transfection into mammalian cells *in vitro* and *in vivo* [1-3]. Mainly, plasmid DNA was condensed by various cationic compounds, such as synthetic cationic polymers, peptides and lipids, which can interact with plasmid DNA electrostatically, in order to be stable for nuclease cleavage and to be effectively delivered into cells [2, 3]. Although the transfection efficiency of plasmid DNA was enhanced using these methods *in vitro*, the cytotoxicity of them is one of problems *in vitro* and *in vivo*. On the other hands, it was reported that when plasmid DNA was directly injected into muscle, liver, and hart *in vivo* [4-6], called as naked plasmid DNA method, the transgene was transiently expressed. Although this method is simple and safe, the level of transgene expression resulting from such local regional administration is relatively low and restricted to the injection site due to its low stability. Therefore, for safer, more stable and efficient gene delivery, it is necessary to condense plasmid DNA with a less cationic material or without one. In our previous study, it was reported that nanoparticles of poly(vinyl alcohol) (PVA) itself or its mixture with plasmid DNA were prepared via hydrogen bonds by ultra-high hydrostatic pressurization, in which the hydrogen bond is strengthen, and were delivered into mammalian cells with low cytotoxicity [7].

In the present study, we hypothesized that the pressure induces the compaction of plasmid DNA itself because DNA is one of typical hydrogen bonding polymers as well as PVA, and then we investigated the effect of pressure on the tertiary structure of plasmid DNA having the super-coiled and relaxed forms. Kunugi et al previously reported that the elevated pressure to 160 MPa induced the super-coiling of relaxed plasmid DNA [8].

RESULTS AND DISCUSSION

First, 1kbp ladder DNA (Takara, Co. Ltd) was used. The ladder DNA solution at the concentration of 20 μg/ml was hydrostatically pressurized at 10,000 atm (980MPa) and 40 °C for 10 min using high pressure machine (Dr.chef, Kobe Steel Co. Ltd). After pressure removal, the obtained solution was analyzed by agarose gel electrophoresis, DLS (Nano-Zs, Malvern Instruments Ltd), CD (J-820, JASCO Co. Ltd) and melting temperature (Tm) at 260 nm (V-560, JASCO Co. Ltd) measurements. There was no change for the agarose gel electrophoresis of the ladder DNA with/without the pressurization, whereas the decrease in the size of the pressurized DNA was confirmed by DLS measurement compared to that of the non-pressurized DNA, suggesting that the compaction of DNA was induced by the pressurization. Also, there were differences between the ladder DNA with and without the pressurization for CD and Tm measurements. These results indicate that the high hydrostatic pressurization affect on the conformation of DNA.

Secondary, plasmid DNA encoding luciferase under T7 promoter (pT7-luc, Promega Co.) was used in order to examine the effect of pressure on the conformational structure of DNA in detail. The aqueous solution of pT7-luc at the concentration of 20 μg/ml was hydrostatically pressurized at 10,000 atm and 40 °C for 20 min. Figure 1 shows the results of DLS measurement of the pT7-luc

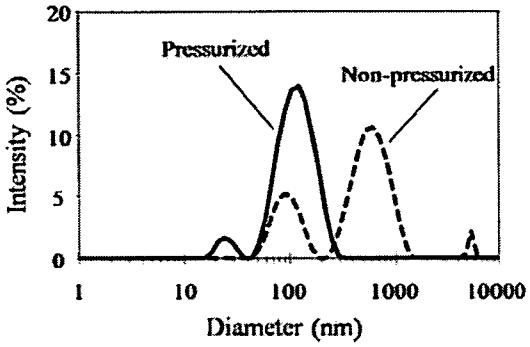

Fig1. DLS measurements of the pT7-luc plasmid DNA with and without the pressurization at 10,000 atm and40 °C for 20 min.

plasmid DNA with and with the pressurization. Before the pressurization, the hydrodynamic diameter of pT7-Luc solution was detected at approximately 95 nm and 625 nm, which were assigned to the super-coiled and relaxed (open-circled) form of pT7-luc plasmid DNA, respectively. After the pressurization, the hydrodynamic diameters of the pT7-luc were measured at approximately 27 nm and 127 nm. It was previously reported that super-coiling of plasmid DNA was induced by elevated pressure to a relaxed plasmid DNA at 160 MPa [8]. Thus, the pT7-luc having the diameter of 127 nm obtained by the pressurization at 10,000 atm was regarded as super-coiling of relaxed pT7-luc plasmid DNA. It is also considered that the super-coiled pT7-luc was effectively condensed by the high pressurization, resulting that the compacted super-coiled pT7-luc was detected at approximately 27 nm.

To examine the conformational change of the pressurized pT7-luc, CD measurement was carried out. There was slight difference in CD spectrum of the pT7-luc with and without pressurization, suggesting that the hydrostatic pressurization also affects on the conformation of plasmid DNA. Furthermore, the stability of the compacted pT7-luc was investigated by digestion test using S1 nuclease, which selectively cleaves single strand DNA. A small amount of the S1 nuclease was required to cleave the compacted pT7-luc than the non-pressurized pT7-luc. It is suggested that the double helix of plasmid DNA could be partly dissociated to single strand by the pressure-induced compaction of plasmid DNA.

To investigate whether the pressurizing strength and time affect the compaction of plasmid DNA, the pT7-luc solution was pressurized at different atmospheres and 40°C for various times. For DLS measurement after pressure removal, the hydrodynamic diameters of the super-coiled and relaxed plasmid DNA were decreased with increasing pressure. Also, at constant pressure at 10,000 atm, a long period of pressure treatment effectively induced the compaction of pT7-luc. These results suggest that the hydrostatic pressurization could regulate the tertiary structure of plasmid DNA.

CONCLUSION

It was found that the high pressurization induced the super-coiling of relaxed plasmid DNA and the compaction of super-coiled plasmid DNA. The extent of the tertiary structural changes of them was depended on the pressurizing strength and time. The high hydrostatic pressurization is considered as a potential tool for preparing the compacted plasmid DNA.

ACKNOWLEDGEMENT

This work was supported by a grant from the Ministry of Health, Labour, and Welfare (MHLW).

REFERENCES

1. Taira, K., Kataoka, K., Niidome, T. editors, Non-viral Gene Therapy Gene Design and Delivery. Tokyo: Springer-Verlag, 2005.
2. Dubruel, P. and Schacht, E. (2006) *Macromolecular Bioscience*, **6**, 789-810.
3. Li, W.J. and Szoka, F.C. (2007) *Pharmaceutical Research*, **24**, 438-449.
4. Budker, V., Zhang, G., Knechtle, S., Wolff, J.A. (1996) GeneTherapy 3, 593–598.
5. Liu, F., Song, Y.K., Liu, D. (1999) *Gene Therapy*, **6**, 1258-1266.
6. Li, K., Welikson, R.E., Vikstrom, K.L., Leinwand, L.A. (1997) *J Mol Cel Cardiol*, **29**, 1499-1504.
7. Kimura, T., Okuno, A., Miyazaki, K., Furuzono, T., Ohya, Y., Ouchi, T., Mutsuo, S., Yoshizawa, H., Kitamura, Y., Fujisato, T., Kishida, A. (2004) *Materials Science and Engineering C*, **24**, 797-801.
8. Tang, G.Q., Tanaka, N., Kunugi, S. (1998) *Biochimica et Biophysica Acta*, **1443**, 364-368.

*Corresponding Author. E-mail: kishida.fm@tmd.ac.jp

Pressure-Induced Molecular Assembly of Hydrogen-Bonded Polymers

SHINGO MUTSUO,[1] KAZUYA YAMAMOTO,[2] TSUTOMU FURUZONO,[3] TSUYOSHI KIMURA,[4] TSUTOMU ONO,[1] AKIO KISHIDA[4]

[1]Department of Material and Energy Science, Graduate School of Environmental Science, Okayama University, Tsushima-Naka, Okayama 700-8530, Japan

[2]Department of Nanostructured and Advanced Materials, Graduate School of Science and Engineering, Kagoshima University, Korimoto, Kagoshima 890-0065, Japan

[3]Department of Biomedical Engineering, National Cardiovascular Center Research Institute, Fujishiro-Dai, Suita, Osaka 565-8565, Japan

[4]Department of Applied Functional Molecules, Institute of Biomaterials and Bioengineering, Tokyo Medical and Dental University, Kanda-Surugadai, Chiyoda-Ku, Tokyo 101-0062, Japan

Received 10 August 2007; accepted 21 December 2007
DOI: 10.1002/polb.21407
Published online in Wiley InterScience (www.interscience.wiley.com).

ABSTRACT: Controlling the noncovalent bondings such as electrostatic interaction, van der Waals force and hydrogen bond, is the key factor to generate molecular assembly. We show that pressure is one of the most intensive variables for controlling these intermolecular forces and producing assembled structure. Macrogel and nanoparticles of hydrogen-bonded polymers were simply obtained through an ultrahigh-pressure process. The morphology of the obtained assembly depends on concentration and various conditions of the pressurization. These results indicate that the ultrahigh-pressure induces inter/intra-hydrogen bond, which is strong enough to maintain microassemblies such as gels and particles. This methodology leads to the molecular design of pressure-induced molecular assembly, and nonharmful processes for molecular separation and drug development. © 2008 Wiley Periodicals, Inc. J Polym Sci Part B: Polym Phys 46: 743–750, 2008

Keywords: crosslinking; hydrogels; nanoparticles; water-soluble polymers

INTRODUCTION

Molecular assembly technology has been gathering interest in the material processing field, especially nanotechnology. Molecular assembly is achieved by noncovalent bonding between adjacent molecules. The development of carbon nanotubes as circuit wires[1,2] and the incorporation of anticancer drugs and amphiphilic polymers into nanomicelles[3,4] are examples of molecular assembly in which noncovalent bonding, such as electrostatic interaction, van der Waals interactions and hydrogen bonds, are well combined.[5–8] Controlling these intermolecular forces is the key factor to create or collapse the assembled structure. Supramolecular chemistry has expanded to allow various elemental molecules to generate elegant assembles,[9–12] whereas the operative factors which regulate molecular assembly are mostly limited by the concentration and/or temperature. Here, we show that

Correspondence to: A. Kishida (E-mail: kishida.fm@tmd.ac.jp)

Journal of Polymer Science: Part B: Polymer Physics, Vol. 46, 743–750 (2008)

pressure, which is one of the most intensive variables in thermodynamics as well as the concentration and temperature,[13–16] can also be used for controlling the intermolecular forces to generate assembled molecules. We found that a poly (vinyl alcohol) (PVA) solution turned into a macrogel or nanoparticle through a simple ultrahigh-pressure process (10,000 atmosphere, 10 min). The morphology of the obtained assembly depended on the PVA concentration, indicating significant inter/intra-molecular hydrogen bonding. Our results demonstrated that ultrahigh-pressure induces hydrogen bonding in water, which is strong enough to maintain microassemblies such as gels and particles.[17,18] Since the interactive potential of molecules is brought out under ultrahigh-pressure, this technology would be applicable to realize the concept for designing assembly molecules proposed by Whitesides and coworkers.[19–21] Furthermore, this methodology leads to the molecular design of pressure-induced molecular assembly, and facilitates nonharmful processes for molecular separation and drug development.

EXPERIMENTAL

Materials

The degree of polymerization of the used PVA (Kuraray, Japan) was 1750. The degree of saponification was 99.8%.

Ultrahigh-Hydrostatic Pressurization

An aqueous PVA solution of predetermined concentration was poured into a plastic bag and was sealed. The bag solution was pressurized using an ultrahigh-pressure machine (hydrostatic pressure). The pressure was set to 1000–10,000 atmospheric pressures, and was processed over the predetermined time period.

Hydrogel Preparation by The Freeze-Thawing Method

An aqueous PVA solution was subjected to five cycles of freeze-thawing, in which the sample was frozen for 12 h at −20 °C, and then thawed for 12 h at 4 °C as one cycle. The mass change of the freeze-thawed sample and the high-pressure processed sample before and after soaking was measured, and the structures of the two gels, both of which had gel ratios over 90%, were compared.

Dynamic Light Scattering Measurement

A 0.5 w/v % PVA solution was high-pressure processed for 10 min at 10,000 atm, and the sample was diluted to an appropriate concentration with ultrapure water, and was subsequently filtered with a 5-μm pore mesh. The particle size was then measured with DLS-7000 (Otsuka Electronics, Japan) using an Ar laser (λ = 488 nm, 75 mW).

Swelling Ratio Measurement

The PVA hydrogel prepared by pressurization was immersed in pure water at room temperature for 10 days and then freeze-dried. The swelling ratio of the PVA hydrogel was calculated as follows:

$$\text{Swelling ratio} = \frac{W_h - W_d}{W_d} \times 100$$

where W_h is the weight of hydrated gel after the dialysis and W_d is the weight of dried gel.

Scanning Electron Microscopy

Observation of PVA assembly was carried out using a scanning electron microscope, S-4700 (Hitachi High Technologies). Specimen for SEM observation was prepared as follows: After a hydrogel was freeze-dried, it was coated with a thin layer of Pt–Pd by the vacuum evaporation technique.

Differential Scanning Calorimetry

DSC measurement was carried out to reveal the melting temperature of PVA assembly. It was carried out at heating rate of 5 °C/min under a constant flow of nitrogen gas.

^{1}H NMR Measurement

The nongelled portion of the pressurized PVA was obtained by the dialysis of the PVA hydrogel. The ^{1}H NMR spectra was obtained by the measurement of the PVA sample dissolved in dimethyl sulfoxide (DMSO-d_6).

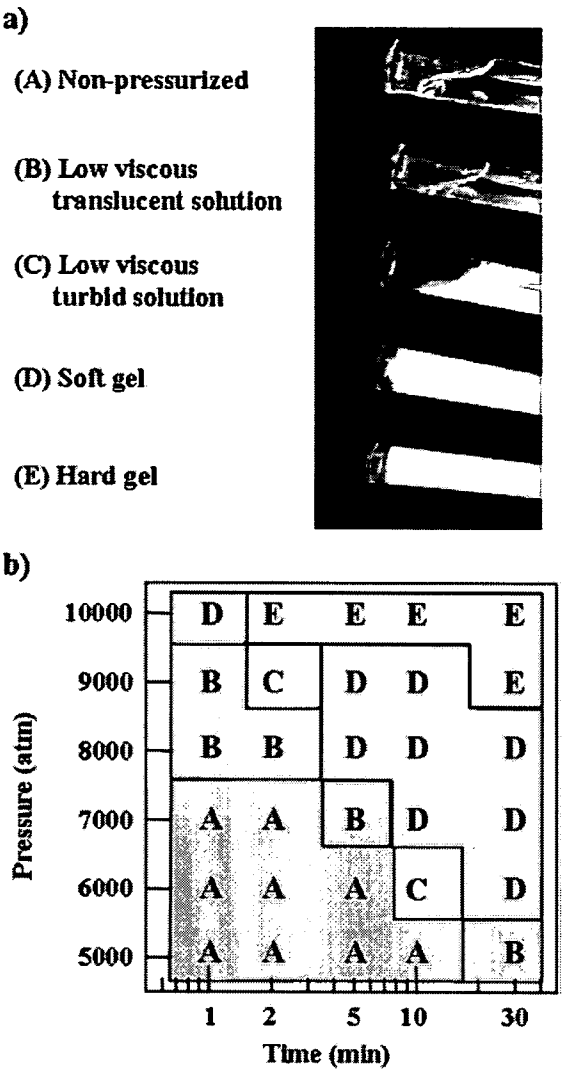

Figure 1. Pressure-induced PVA assembly. (a) Photographs of a 10 w/v% PVA solution pressurized under various conditions: (A) nonpressurized, (B) 7000 atm, 1 min, (C) 9000 atm, 1 min, (D) 7000 atm, 10 min, and (E) 10000 atm, 10 min. (b) Phase (constitutional) diagram of a 5 w/v % PVA solution pressurized under various conditions. The state was decided by visual observation according to the photographs. [Color figure can be viewed in the online issue, which is available at www.interscience.wiley.com.]

RESULTS AND DISCUSSION

PVA Assembly Formed by Pressurization

Aqueous solutions of PVA at 1–20 w/v % concentrations were pressurized hydrostatically under various conditions. Figure 1(a) shows photographs of typical samples of 10 w/v % PVA solutions pressurized at different atmosphere pressure (atm) for 10 min. A translucent solution, the precipitate and hydrogel of PVA was obtained by increasing the pressure, indicating that the assembly of PVA molecules was induced by pressure treatment. The hydrogel was stable in pure water, and the yield (gelation ratio) was 90% or more. It is well-known that PVA solutions transform into hydrogels when the solution was frozen and thawed sequentially several times; this procedure is called the freeze-thawing method. Approximately 10 days is required to form a hydrogel with similar strength as a hydrogel obtained by pressurization for only 10 min. Thus, this simple pressurizing method can be expected to be an energy saving process. The influence of the pressure conditions on the formation of a PVA assembly was examined using a PVA solution of 5 w/v % in detail. Figure 1(b) shows the state diagram of the PVA assembly in a pressure–time plot determined by visual observation according to the photographs shown in Figure 1(a). The translucent solution and hydrogel were acquired by pressure treatment at more than 8000 atm over a very short time (one min). The tendency for gelation of PVA with increasing pressure was observed for each step of pressurization. In addition, at constant pressure, a long period of pressure treatment induced assembly of the PVA, even in the case of only 6000 atm, and the hydrogel was obtained by pressurization for 30 min. Furthermore, DLS measurements of a 10 w/v % solution pressurized under conditions in which a hydrogel was not obtained revealed the formation of PVA nanoassembly and the

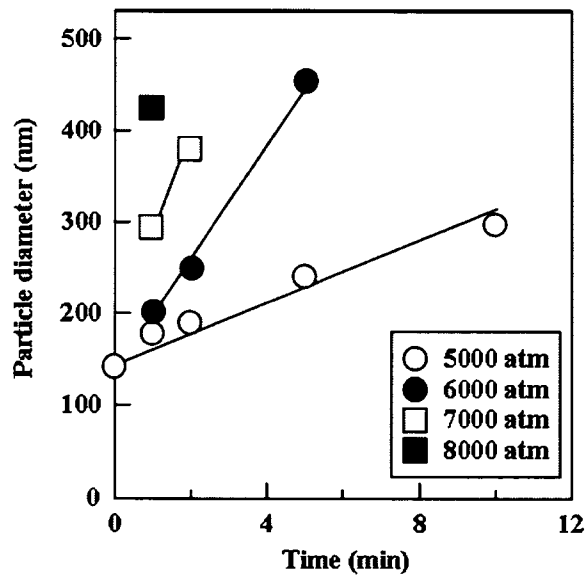

Figure 2. DLS measurements of a 10 w/v % PVA solution pressurized under various conditions.

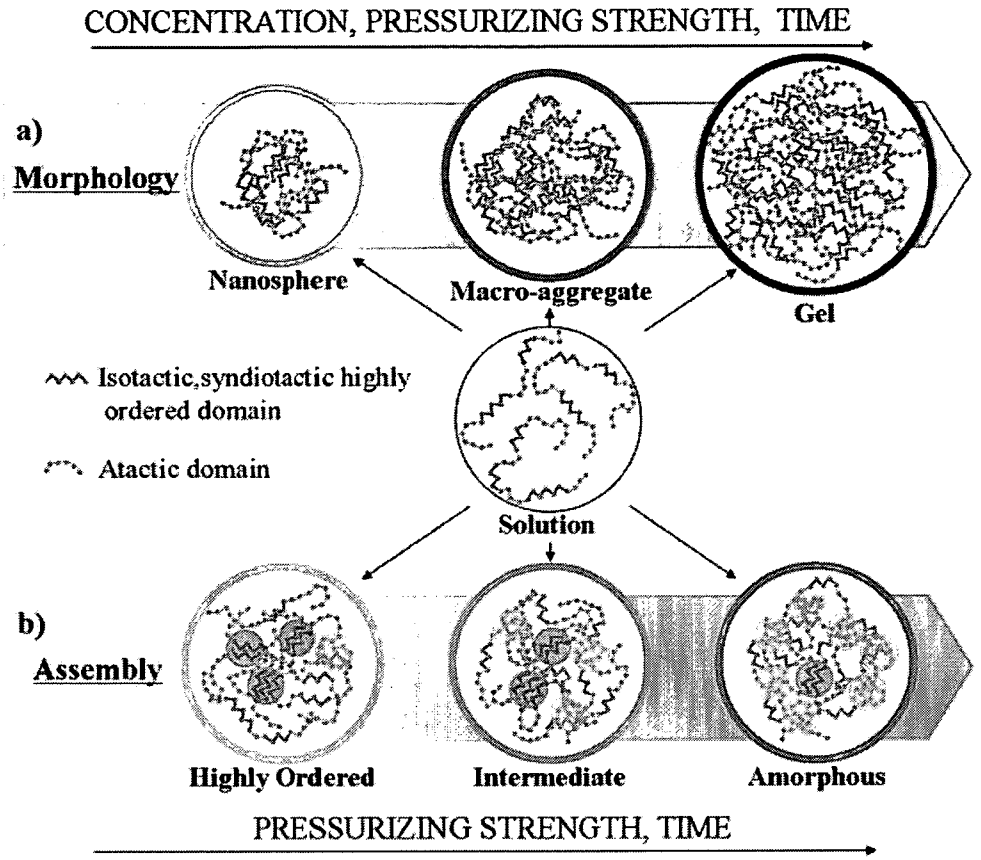

Figure 3. Illustration of the mechanism of hydrogen-bonding polymer assembly induced by ultrahigh-pressurization. (a) Effect of conditional parameters on the morphology of PVA assembly. (b) Effect of secondary structure of PVA on the formation of molecular assembly.

growth of the PVA nanoassembly under prolonged periods of pressure (Fig. 2). From these results, it is clear that the assembly of PVA at nanometer size was promoted under pressure conditions of higher pressure and a longer incubation period, and could be controlled by altering the pressurizing strength and time [Fig. 3(a)].

Characteristics of PVA Assembly Formed By Pressurization

The gelation of a PVA solution at 5, 10, 15, and 20 w/v % concentrations was also achieved by pressurization at 10,000 atm. The swelling ratio of the obtained hydrogel was determined by the starting concentration of the PVA solution, and showed a constant value for all concentrations when they were treated at 10,000 atm for more than 10 min (Fig. 4). On the other hand, the swelling ratio of the obtained hydrogel at 5 min of pressurizing time was inversely proportional to the concentration of the PVA solution (Fig. 5). This result indicates that a tight interaction

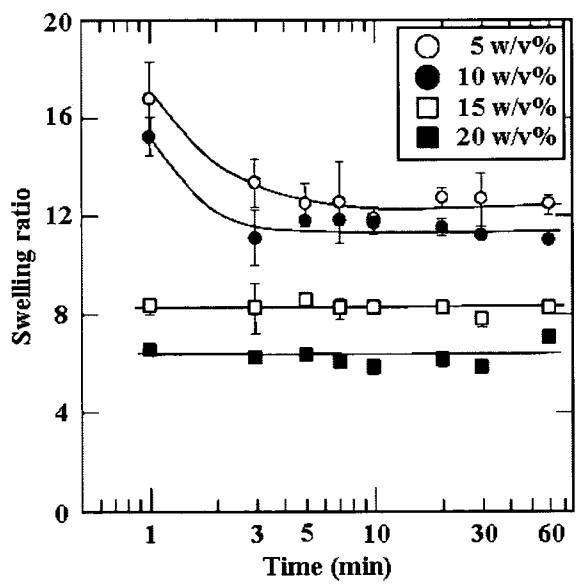

Figure 4. Effect of PVA concentration on swelling ratio of PVA hydrogel formed by pressurization at 10,000 atm for various minutes.

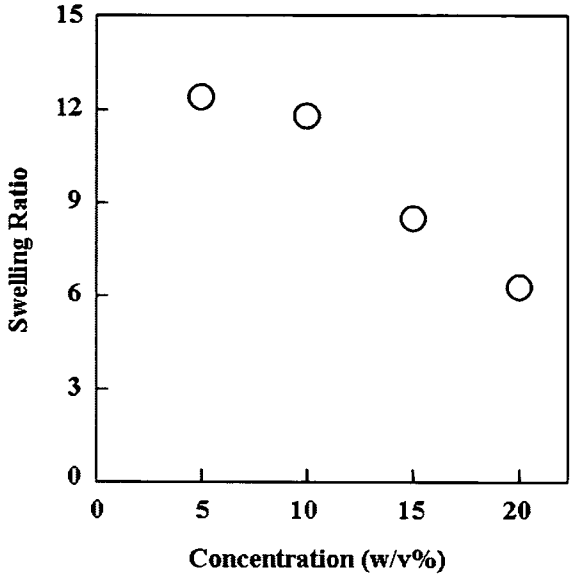

Figure 5. Swelling ratio of PVA hydrogels formed by pressurization at 10,000 atm for 5 min.

between the PVA molecules was formed with increasing the concentration of PVA solution. The interior structure of the PVA hydrogel pressurized at 10,000 atm for 10 min was observed with a SEM (Fig. 6). A mesh-like structure with pores of about 300 nm was observed for the hydrogel obtained by the pressure treatment of a 5 w/v % PVA solution. The mesh-like structures with smaller pores were formed upon increasing the PVA concentration. As the pressure treatment was carried out at 40 °C, no ice crystal was formed.[22] That is, ice crystals did not affect the mesh-like structures formed by the high-pressure process. In contrast, in the case of the freeze-thawing method, the mesh-like structures were formed by the formation of ice crystals. Therefore, a different process of formation between the two methods was suggested.

DSC analysis of the PVA hydrogels let us know the melting temperature of the associated PVA molecules. The relaxation, which occurs at a temperature between 200 and 260 °C, is caused by the melting of the crystalline domains of PVA.[23,24] The increase of intermolecular hydrogen bonding in PVA raises the melting temperature, leading to a high heat resistance.[25] The melting temperature of the PVA hydrogel

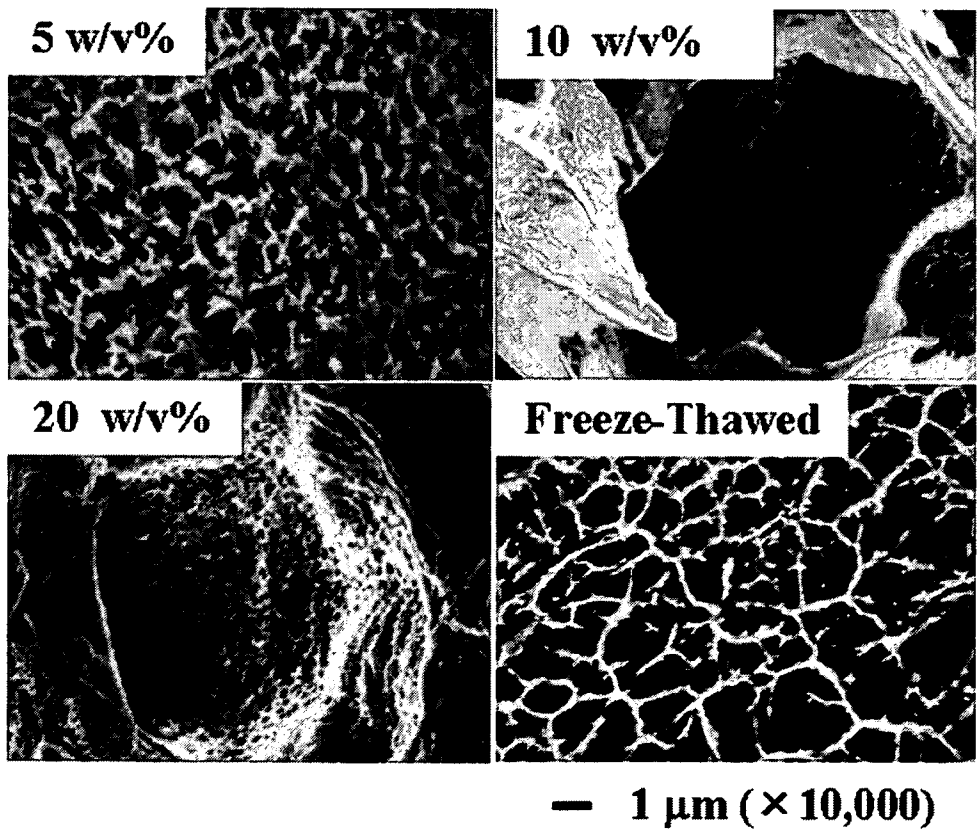

Figure 6. SEM images of PVA hydrogels of 5, 10, and 20 w/v % formed by pressurization at 10,000 atm for 10 min and 5 w/v % PVA hydrogels formed by the freeze-thawing method.

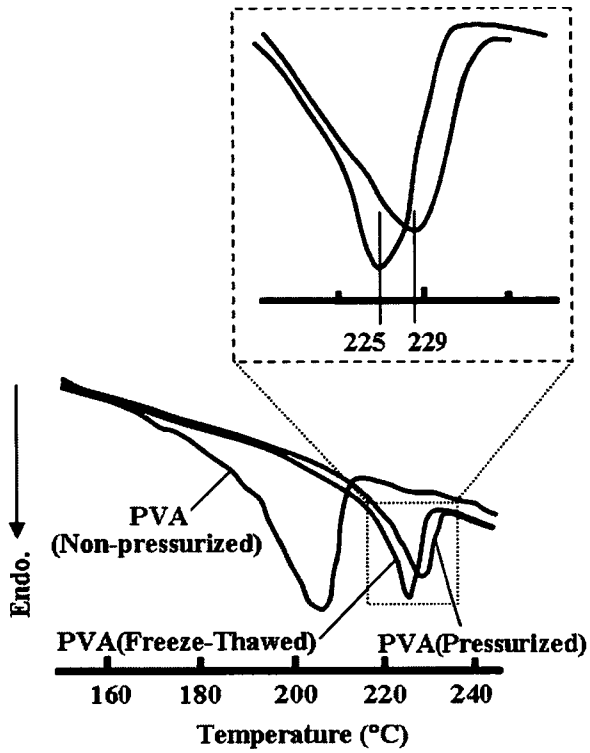

Figure 7. DSC measurements of PVA hydrogels formed by pressure treatment or the freeze-thawing method.

obtained by high-pressure process was higher than that of the hydrogel prepared by the freeze-thawing method (Fig. 7). This result indicates that high-pressure process could form stronger intermolecular interactions in PVA than the freeze-thawing method. Although we need to go into additional details about the thermodynamic stability of the PVA hydrogel obtained by high-pressure process, we have only limited information about it.

Many researchers have examined the self-organization of molecules in an aqueous environment, because the hydrogen bonds and hydrophobic interactions were able to act as a driving force for structure formation.[26–29] The formation and deformation of the hydrogen bonds in an aqueous environment can be controlled by changing the temperature and ionic concentration. The effect of the salt concentration on the high-pressure process of the PVA solution was then examined. When the NaCl concentration was increased, the PVA hydrogel was obtained even at low pressure (around 6000 atm). At over 9000 atm, stable PVA hydrogels were obtained at any salt concentration, and the swelling ratio was almost constant (Fig. 8).

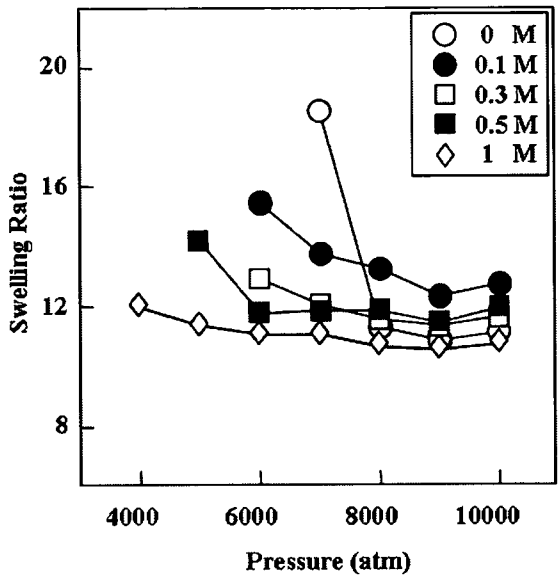

Figure 8. Swelling ratio of 10 w/v% PVA hydrogels formed by pressurization at 10,000 atm for 5 min with various salt concentrations.

When PVA solutions of less than 1 w/v % concentration were treated with pressurization at 10,000 atm, clear and turbid solutions were obtained, as well as in the case of a 10 w/v % PVA solution pressurized under low atmospheric pressure for a short time. The formation of small particles with a diameter of about 200–400 nm was confirmed from SEM observation and DLS measurements (Fig. 9). As a result, it was believed that the formation of intra/inter-molecular hydrogen bonds is the first step in the initial structural formation of PVA, and afterward the size and morphology of the structure is determined in proportion to the concentration of the solution.

The effect of the secondary (atactic, syndiotactic, and isotactic) structure of PVA molecule was observed by the ^{1}H NMR spectra analysis for the nongelled portion of the pressurized PVA solution (Table 1). Short-time pressurizing treatment at

Table 1. NMR Analysis of the Nongelled Portion of the Pressurized PVA Solution

	Tacticity		
	mm	mr	rr
PVA117HC	22.6	47.6	29.8
S-PVA	11.9	49.9	38.2
PVA117HC (20%, 6000 atm, 5 min)	21.4	49.0	29.6
PVA117HC (20%, 6000 atm, 10 min)	33.8	37.7	28.5
PVA117HC (10%, 7000 atm, 5 min)	20.9	48.0	31.1

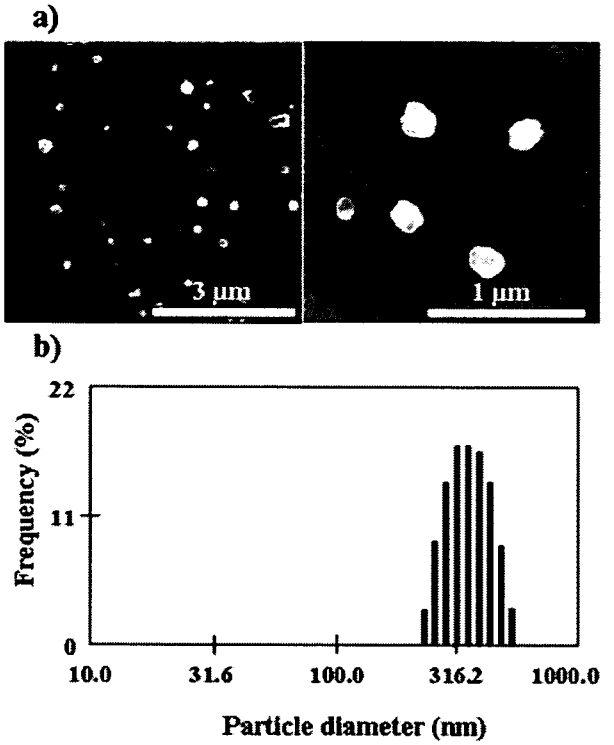

Figure 9. Small aggregates formation of PVA by pressurization. (a and b) SEM images and DLS measurements, respectively, of PVA particles formed by pressurizing a 0.5 w/v % PVA solution at 10,000 atm for 10 min.

6000 atm had no effect on the content of the secondary structure of PVA molecule, whereas after the longer treatment (10 min), the decrease of the atactic portion (mr) of PVA molecule was observed. There was no free PVA after more than 20-min treatment. These results indicated that the atactic PVA was gelled prior to other kinds of the stereostructured PVA, and after prolonged treatment all kinds of stereostructured PVA gelled. These differences of aggregation ability of each stereostructured PVA could be applicable to form the ordered structure by changing treatment time, pressure, and the content of each secondary structures of PVA [Fig. 3(b)].

The High-Ordered Structure of PVA Assembly

The assembly of PVA depended on the strength and period of pressurization and the PVA concentration. It should be noted that molecular assembly is formed through two processes induced by pressurization, which are dehydration and the subsequent formation of hydrogen bonds among inter/intra-molecules. Indeed, it is believed that under pressurized conditions, the hydration shell of the PVA molecules was disrupted, and then hydrogen bonding interactions between the hydroxyl groups of the PVA were formed. Thus, the gelation of PVA was promoted by increasing the pressure. It seems that the reaction could proceed with a long duration of pressurization even at moderate pressures. With regard to the concentration-assembly relationship, monodispersed and nanometer-scale structures were formed by intramolecular interactions under dilute conditions, whereas the macrostructure (larger than mm) was formed by the intermolecular interactions between nanometer-scaled structures which contained molecular entanglements under concentrated conditions. To construct a well-defined molecular assembly, it is necessary to optimize the primary chemical structure of the polymer molecules, and to fabricate molecules with a specific structure by exploiting various interactions. The intermolecular force maintaining the structure of the supramolecular assembly includes van der Waals force, electrostatic interactions, hydrophobic interactions, and hydrogen bonds, etc. The individual interaction energy of a hydrogen bond is small, while if it interacts along the chain direction, hydrogen bond is able to maintain a huge PVA hydrogel by assembling high-molecular weight PVA moieties. The most important factor that influences the structure formation induced by high pressure is the chain length and the secondary structure of the PVA molecule, as well as the temperature, concentration, and ionic concentration. Controlling the factors, it is expected that the ordered structures of molecular assembly can be generated. In a conventional technique, changing the concentration of the solution or a substitution of the solvent makes it difficult to change the molecular-assembly situation gradually. On the other hand, the pressuring conditions can be reversibly controlled and highly controlled operation for molecular assembly by building the interactive part, which works at a different pressure in the molecules. In the case where two or more hydrogen bonding functional groups are present, the control of a higher-order structure can be achieved by pressurizing in a stepwise fashion. We assumed that the secondary structure of PVA is one of the most possible candidates for the factors for obtaining the ordered molecular assembling structure. It is expected that such technology can be applied to build a structure by the manipulating molecular interactions to develop

novel structure in aqueous solution, leading to new science and technology.

CONCLUSIONS

The PVA assembly was simply obtained through an ultrahigh-pressure process. The morphology of PVA assembly depended on the strength and period of pressurization, the PVA concentration, the PVA chain length, and the PVA secondary structure. Under the ultrahigh-pressure, molecular assembly is formed through two processes, which are dehydration and the subsequent formation of hydrogen bonds among inter/intramolecules. Thus, the ultrahigh-pressure process can manipulate molecular interactions. Therefore, it is expected that the novel high-ordered structures based on molecular assembly can be generated by controlling various factors in an ultrahigh-pressure process.

This work was partly supported by Kuraray Co., for their supply of the poly(vinyl alcohol).

REFERENCES AND NOTES

1. Joachim, C.; Gimzewski, J. K.; Aviram, A. Nature 2000, 408, 541–548.
2. Cui, Y.; Lieber, C. M. Science 2001, 291, 851–853.
3. Yokoyama, M.; Miyauchi, M.; Yamada, N.; Okano, T.; Sakurai, Y.; Kataoka, K.; Inoue, S. Cancer Res 1990, 50, 1693–1700.
4. Nishiyama, N.; Kataoka, K. Pharmacol Ther 2006, 112, 630–648.
5. Bong, D. T.; Clark, T. D.; Granja, J. R.; Ghadiri, M. R. Angew Chem Int Ed 2001, 40, 988–1011.
6. Chandler, D. Nature 2005, 437, 640–647.
7. Tanaka, T.; Tasaki, T.; Aoyama, Y. J Am Chem Soc 2002, 124, 12453–12462.
8. Zemb, T. Curr Opin Colloid Interface Sci 2003, 8, 1–4.
9. Lehn, J. M. Proc Natl Acad Sci USA 2002, 99, 4763–4768.
10. Prins, L. J.; De Jong, F.; Timmerman, P.; Reinhoudt, D. N. Nature 2000, 408, 181–184.
11. Barth, J. V.; Weckesser, J.; Lin, N.; Dmitriev, A.; Kern, K. Appl Phys A: Mater Sci Process 2003, 76, 645–652.
12. Balzani, V.; Credi, A.; Raymo, F. M.; Stoddart, J. F. Angew Chem Int Ed 2000, 39, 3348–3391.
13. Mozhaev, V. V.; Heremans, K.; Frank, J.; Masson, P.; Balny, C. Proteins: Struct Funct Genet 1996, 24, 81–91.
14. Kunugi, S.; Yoshida, D.; Kiminami, H. Colloid Polym Sci 2001, 279, 1139–1143.
15. Otero, L.; Sanz, P. D. J Food Sci 2003, 68, 2523–2528.
16. Kalichevsky-Dong, M. T.; Ablett, S.; Lillford, P. J.; Knorr, D. Int J Food Sci Technol 2000, 35, 163–172.
17. Kunugi, S.; Takano, K.; Tanaka, N.; Suwa, K.; Akashi, M. Macromolecules 1997, 30, 4499–4501.
18. Seto, Y.; Kameyama, K.; Tanaka, N.; Kunugi, S.; Yamamoto, K.; Akashi, M. Colloid Polym Sci 2003, 281, 690–694.
19. Bowden, N.; Terfort, A.; Carbeck, J.; Whitesides, G. M. Science 1997, 276, 233–235.
20. Breen, T. L.; Tien, J.; Oliver, S. R. J.; Hadzic, T.; Whitesides, G. M. Science 1999, 284, 948–951.
21. Whitesides, G. M.; Crzybowski, B. Science 2002, 295, 2418–2421.
22. Chou, I. M.; Blank, J. G.; Goncharov, A. F.; Mao, H. K.; Hemley, R. J. Science 1998, 281, 809–812.
23. Nugent, M. J. D.; Higginbotham, C. L. Eur J Pharm Biopharm 2007, 67, 377–386.
24. Hassan, C. M.; Ward, J. H.; Peppas, N. A. Polymer 2000, 41, 6729–6739.
25. Nagara, Y.; Nakano, T.; Okamoto, Y.; Gotoh, Y.; Nagura, M. Polymer 2001, 42, 9679–9686.
26. Arnaud, A.; Belleney, J.; Boue, F.; Bouteiller, L.; Carrot, G.; Wintgens, V. Angew Chem Int Ed 2004, 43, 1718–1721.
27. Kim, C.; Lee, S. J.; Lee, I. H.; Kim, K. T.; Song, H. H.; Jeon, H. J. Chem Mater 2003, 15, 3638–3642.
28. Kawasaki, T.; Tokuhiro, M.; Kimizuka, N.; Kunitake, T. J Am Chem Soc 2001, 123, 6792–6800.
29. Roy, S.; Dey, J. Langmuir 2003, 19, 9625–9629.

Controlling Coupling Reaction of EDC and NHS for Preparation of Collagen Gels Using Ethanol/Water Co-Solvents

Kwangwoo Nam, Tsuyoshi Kimura, Akio Kishida*

To control the crosslinking rate of the collagen gel, ethanol/water co-solvent was adopted for the reaction solvent for the collagen microfibril crosslinking. Collagen gel was prepared by using EDC and NHS as coupling agents. Ethanol did not denaturate the helical structure of the collagen and prevented the hydrolysis of EDC, but showed the protonation of carboxylate anions. In order to control the intra- and interhelical crosslink of the collagen triple helix, variations of the mole ratio of carboxyl group/EDC/NHS, and of the ethanol mole concentration were investigated. Increase in the EDC ratio against the carboxyl group increased the crosslinking rate. Furthermore, an increase in the ethanol mole concentration resulted in an increase of the crosslinking rate until ethanol mole concentration was 0.12, but showed gradual decrease as the ethanol mole concentration was further increased. This is because the adsorption of solvent by the collagen gel, protonation of carboxylate anion, and hydrolysis of EDC is at its most optimum condition for the coupling reaction when the ethanol mole concentration is 0.12. The re-crosslinking of the collagen gel showed an increase in the crosslinking rate, but did not show further increase when the coupling reaction was executed for the third time. This implied that the highest possible crosslinking rate for the intra- and interhelical is approximately 60% when EDC/NHS is used.

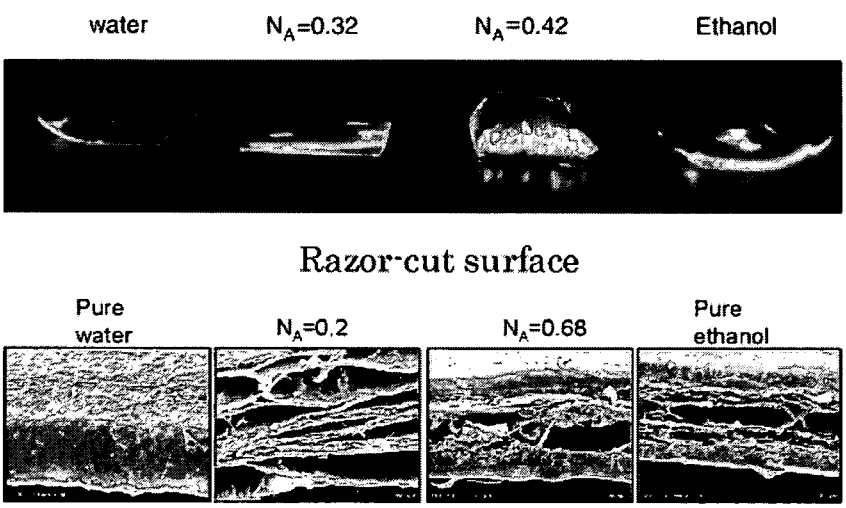

Introduction

The construction of an extracellular matrix (ECM) using natural products has been performed by many researchers worldwide. Based on the fact that an ECM is mainly composed of collagen and elastin, many researchers have

K. Nam, T. Kimura, A. Kishida
Division of Biofunctional Molecules, Institute of Biomaterials and Bioengineering, Tokyo Medical and Dental University, 2-3-10 Kanda-Surugadai, Chiyoda-ku, Tokyo 101-0062, Japan
Fax: 03-5280-8029; E-mail: kishida.fm@tmd.ac.jp

Macromol. Biosci. **2008**, *8*, 32–37

DOI: 10.1002/mabi.200700206